

Phase Behavior of Poly(2-vinylpyridine)-*block*-poly(4-vinylpyridine) Copolymers

Sung Hyun Han, Dong Hyun Lee, and Jin Kon Kim*

National Creative Research Initiative Center for Block Copolymer Self-Assembly, Department of Chemical Engineering, Pohang University of Science and Technology, Pohang, Kyungbuk 790-784, Republic of Korea

Received May 17, 2007

Revised Manuscript Received July 6, 2007

Introduction

The phase behavior of block copolymers with various microdomains has been investigated extensively by many research groups.^{1–5} Most block copolymers exhibit order-to-disorder transition (ODT) upon heating because of the decrease in the enthalpic repulsive interactions between constituent segments. The phase behavior of block copolymers depends on the volume fraction (f) of one block, the degree of polymerization (N), and the Flory–Huggins segmental interaction parameter (χ).²

Block copolymers containing poly(2-vinylpyridine) (P2VP) or poly(4-vinylpyridine) (P4VP) have been extensively studied^{6–10} because they can be useful to prepare nanoparticles,^{11,12} nanofibers,¹³ or photonic band-gap materials.¹⁴ Many research groups have reported on the interaction parameter (χ) between the polystyrene (PS)/P2VP and/or PS/P4VP pairs.^{6,15–18} Among many expressions (or values) of χ for PS/P2VP and PS/P4VP available in the literature, Zha et al.¹⁸ obtained a comprehensive expression for temperature-dependent χ (or the interaction energy density α in the unit of mol/cm³) using small-angle X-ray scattering (SAXS) on low-molecular-weight polystyrene-*block*-poly(2-vinylpyridine) (PS-*b*-P2VP) copolymer and polystyrene-*block*-poly(4-vinylpyridine) (PS-*b*-P4VP) copolymer exhibiting disordered state over the entire range of experimental temperatures investigated. It was found that for comparable molecular weights and block compositions ODT temperature (T_{ODT}) and χ (or α) of PS-*b*-P4VP copolymer are much higher than those of PS-*b*-P2VP copolymer.¹⁸ This is because the dipole polarization of PS-*b*-P4VP copolymer is greater than that of PS-*b*-P2VP copolymer.¹⁸

If this is the case, P2VP and P4VP would not be miscible. Grosius et al.¹⁹ first synthesized poly(2-vinylpyridine)-*block*-poly(4-vinylpyridine) (P2VP-*b*-P4VP) copolymer by anionic polymerization. After fractionation of the P2VP-*b*-P4VP copolymers synthesized using solvent/nonsolvent mixtures, they investigated the domain spacing of the fractionated P2VP-*b*-P4VP copolymers in various solvents. However, they did not investigate the T_{ODT} of the P2VP-*b*-P4VP copolymers and the segment–segment interactions (χ or α) of the P2VP/P4VP pair.

Very recently, we investigated the phase behavior of P2VP-*b*-P4VP copolymers using SAXS, rheometry, and static birefringence. For the study, we prepared via anionic polymerization P2VP-*b*-P4VP copolymers with various molecular weights and block length ratios. We also determined temperature-dependent interaction parameters (α) for P2VP/P4VP pair by obtaining

SAXS profiles of a low-molecular-weight P2VP-*b*-P4VP copolymer at various temperatures and curve fitting to the random phase approximation (RPA) theory.² Quite interestingly, we found that P2VP-*b*-P4VP copolymer underwent ODT upon heating, similar to PS-*b*-P2VP and PS-*b*-P4VP copolymers. This observation indicates that the repulsive force between P2VP and P4VP becomes significant enough to induce microphase separation in relatively low molecular weights ($\sim 6\,000$) of symmetric P2VP-*b*-P4VP copolymer even though the only difference between P2VP and P4VP is the position of nitrogen in the pyridine ring (ortho vs para positions). We also found that the value of α for P2VP/P4VP pair lies between that for PS/P4VP and PS/P2VP pairs.

Experimental Section

P2VP-*b*-P4VP copolymers with various molecular weights and block length ratios were synthesized by sequential anionic polymerization of 2-vinylpyridine (2VP) and 4-vinylpyridine (4VP) in tetrahydrofuran at $-78\text{ }^{\circ}\text{C}$ under purified argon atmosphere using *sec*-butyllithium (BuLi) initiator. Before the polymerization of 4VP, 1,1-diphenylethylene was attached to the end of the living P2VP anion to avoid a side reaction during the initiation of 4VP by *sec*-BuLi. The weight- and number-average molecular weights, M_w and M_n , respectively, were measured by size exclusion chromatography using P2VP standards in dimethylformamide (DMF) solution, and the weight fraction of P2VP block was determined by ¹H nuclear magnetic resonance spectroscopy. The molecular characteristics of the P2VP-*b*-P4VP copolymers synthesized are summarized in Table 1.

SAXS measurements were performed on beamlines 4C1 and 4C2 at the Pohang Light Source (Korea), where a W/B4C double multilayer delivered monochromatic X-rays on the samples with a wavelength of 0.1608 nm.²⁰ A 2-D CCD camera (Princeton Instruments, SCX-TE/CCD-1242) was used to collect the scattered X-rays. All samples were prepared by molding at 200 $^{\circ}\text{C}$ (which is higher than the glass transition temperatures of P2VP and P4VP blocks) and annealing at the same temperature under vacuum for 48 h. The sample was sandwiched by polyimide films to prevent it from flowing at high temperatures. Then, it was inserted into a heating block circulating with nitrogen to prevent thermal degradation. The heating rate was 0.5 $^{\circ}\text{C}/\text{min}$. We were able to measure the SAXS intensity of P2VP-*b*-P4VP copolymers, although the monomeric molecular weight of P2VP is the same as that P4VP. This is because synchrotron SAXS could measure an electron density contrast between P2VP and P4VP block, though small, arising from different the mass densities of P2VP and P4VP.¹⁸ However, this difference could not be detected by transmission electron microdomain whether the sample was stained by iodine or not. We also measured the absolute SAXS intensity of a low-molecular-weight P2VP-*b*-P4VP copolymer at various temperatures with an exposure time of 125 s, as described in detail in the previous paper.¹⁸

An advanced Rheometric expansion system (ARES, TI Instruments) with a parallel-plate fixture (25 mm diameter) was used to measure the dynamic storage and loss moduli (G' and G'') of P2VP-*b*-P4VP copolymers at a heating rate of 0.5 $^{\circ}\text{C}/\text{min}$. A strain amplitude of 0.05 and angular frequency of 0.1 rad/s were used. Depolarized transmitted light (static birefringence)^{21,22} was also used to determine the T_{ODT} of all P2VP-*b*-P4VP copolymers synthesized in this study. Vertically polarized light from a He–Ne laser passed through the sample and a horizontal polarizer onto a photodiode. Samples with a thickness of 1.0 mm and a diameter of 5 mm were covered by two glass slides and then subjected to heating at a rate of 1.0 $^{\circ}\text{C}/\text{min}$. We found that no thermal degradation occurred for all the samples even after the SAXS, rheology, and

* To whom correspondence should be addressed: e-mail jkkim@postech.ac.kr.

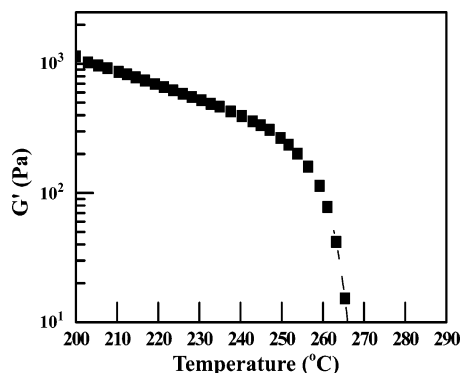


Figure 1. (a) Temperature dependence of G' at $\omega = 0.1$ rad/s for P24VP-L.

Table 1. Molecular Characteristics of P2VP-*b*-P4VPs Employed in This Study

sample code	M_w^a	M_w/M_n	w_{P2VP}^b	remark
P24VP-LMW	5410	1.16	0.42	fully disordered
P24VP-LD	3940	1.21	0.54	fully disordered
P24VP-LO	7030	1.13	0.48	fully ordered
P24VP-L	5950	1.19	0.54	$T_{ODT} = 266$ °C
P24VP-CD	3430 ^c	1.12	0.72	fully disordered
P24VP-CO	19410 ^c	1.12	0.72	fully ordered
P24VP-C	8750 ^c	1.15	0.7	$T_{ODT} = 222$ °C

^a Measured by SEC using P2VP standards in DMF. ^b Measured by ¹H NMR. ^c Determined M_n from ¹H NMR and M_w using M_w/M_n from SEC using P2VP standards in DMF.

birefringence measurement, since M_w and M_w/M_n of samples did not change.

Results and Discussion

Figure 1 gives the temperature dependence of G' during the dynamic temperature sweep experiment at $\omega = 0.1$ rad/s for P24VP-L, showing initially a gradual decrease in G' until reaching about 260 °C and then a precipitous drop at a temperature close to 266 °C. Since a precipitous decrease in G' signifies the onset of ODT,²³ we regard the T_{ODT} of P24VP-L to be 266 °C.

Figure 2a gives SAXS profiles (plots of intensity $I(q)$ vs scattering vector q defined by $q = (4\pi/\lambda) \sin(\theta/2)$ with θ and λ being the scattering angle and the wavelength of the incident beam, respectively) of P24VP-L at various temperatures. It is seen from Figure 2a that a sharp peak is observed up to 260 °C, and then a broad peak is observed at temperatures higher than 266 °C due to the correlation hole effect. Thus, the T_{ODT} of P24VP-L is determined to be 266 °C. From Figure 2a we prepared plots of the reciprocal of the maximum scattering intensity $1/I_m(q^*)$, with q^* being the scattering angle at the scattering maximum, and the full width at half-maximum of the peak (fwhm) vs the inverse of the absolute temperature ($1/T$), as shown in Figure 2b. From Figure 2b we also determine the T_{ODT} of P24VP-L to be about 266 °C, which is in good agreement with the T_{ODT} determined from Figure 1. Since P24VP-L has a symmetric block composition (see Table 1), we conclude that it has lamellar microdomains in an ordered state. It is interesting to observe that the symmetric P2VP-*b*-P4VP copolymer having such low molecular weight (~ 6000) exhibits ODT.

We found that when the M_w of symmetric P24VP was increased to 7030 (P24VP-LO), its T_{ODT} was above 300 °C, the highest experimentally accessible temperature before the

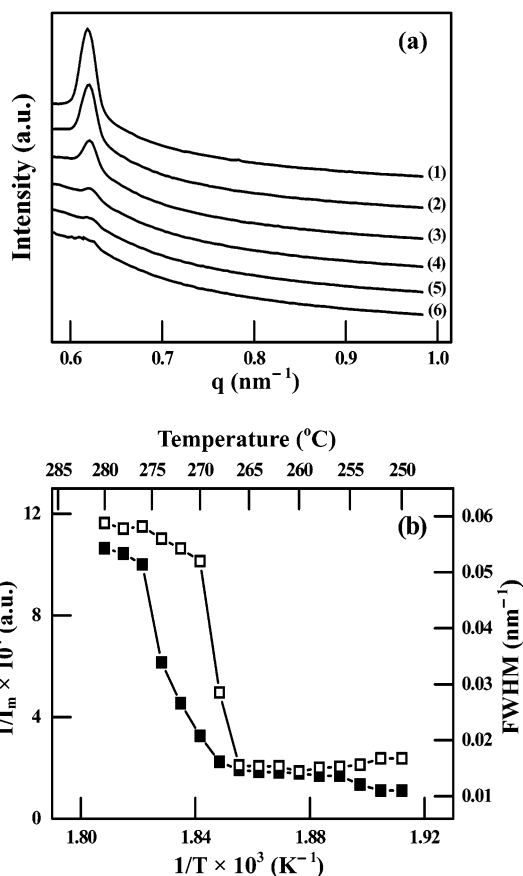


Figure 2. (a) SAXS profiles of P24VP-L at various temperatures (°C): (1) 252, (2) 256, (3) 260, (4) 266, (5) 268, and (6) 272. (b) plots of $1/I_m(q^*)$ vs $1/T$ (■) and plots of fwhm vs $1/T$ (□) for P24VP-L.

onset of thermal degradation, while when the M_w of symmetric P24VP was decreased to 3940 (P2VP-LD), it remained in the disordered state over the entire range of temperatures investigated (see Figure S1 in the Supporting Information).

Figure 3a gives the temperature dependence of G' at $\omega = 0.1$ rad/s for P24VP-C, showing initially a gradual decrease in G' until reaching about 210 °C and then a precipitous drop at a temperature close to 220 °C. Figure 3b gives plots of $1/I_m(q^*)$ and fwhm vs $1/T$, from which we determine the T_{ODT} of P24VP-C to be 222 °C, which is in good agreement with the T_{ODT} determined from Figure 3a. The SAXS profiles at various temperatures are given in Figure S2 in the Supporting Information. Although the microdomains of P24VP-C could not be determined by SAXS due to the lack of higher order peaks, we conclude that it has cylindrical microdomains (see Table 1 for the block composition of P24VP-C), which is supported by the existence of birefringence (see Figure S3 in the Supporting Information). We have found that P24VP-CO with $w_{P2VP} = 0.72$ and $M_w = 19410$ is in an ordered state, while P24VP-CD with $w_{P2VP} = 0.7$ and $M_w = 8750$ is in the disordered state over the entire range of temperatures investigated up to 300 °C (see Figure S4 in the Supporting Information).

Figure 4a gives the structure factor $S(q)$ which was obtained from the absolute SAXS intensities ($d\Sigma(q)/d\Omega$ with units of cm^{-1}) of P24VP-LMW at various temperatures, showing that it is in the disordered state over the entire range of temperatures investigated. The calculation of α ($= \chi/V_{\text{ref}}$ with V_{ref} being the reference monomeric volume) at various temperatures was obtained from the curve-fitting of SAXS intensity to the Leibler mean-field theory. The details of the procedures employed are

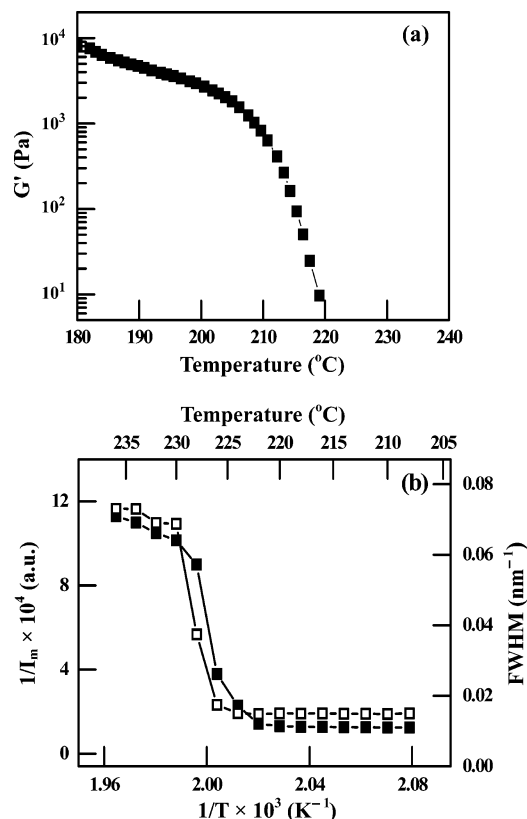


Figure 3. (a) Temperature dependence of G' at $\omega = 0.1$ rad/s and (b) plots of $1/I_m(q^*)$ vs $1/T$ (■) and plots of fwhm vs $1/T$ (□) for P24VP-C.

referred to a recent paper.¹⁸ For the curve fitting, we employed the following expressions for the temperature-dependent specific volumes (cm^3/g) of P2VP and P4VP.¹⁸

$$\nu_{\text{P2VP}} = 0.874 + 1.284 \times 10^{-4} (T - 273) \quad \text{for } T < 373 \text{ K} \quad (1a)$$

$$\nu_{\text{P2VP}} = 0.852 + 3.752 \times 10^{-4} (T - 273) \quad \text{for } T > 373 \text{ K} \quad (1b)$$

$$\nu_{\text{P4VP}} = 0.896 + 1.052 \times 10^{-4} (T - 273) \quad \text{for } T < 423 \text{ K} \quad (2a)$$

$$\nu_{\text{P4VP}} = 0.851 + 4.174 \times 10^{-4} (T - 273) \quad \text{for } T > 423 \text{ K} \quad (2b)$$

By repeating the same procedure at different temperatures for the SAXS profiles of P24VP-LMW, we prepared plots of α vs $1/T$ as given in Figure 4b, from which we obtain the following expression for the temperature-dependent interaction parameter α (mol/cm^3):

$$\alpha_{\text{P2VP/P4VP}} = 1.64 \times 10^{-3} + 0.236/T \quad (3)$$

In Figure 4b, we have added two additional plots of α vs $1/T$ for $\alpha_{\text{PS/P2VP}}$ and $\alpha_{\text{PS/P4VP}}$, which were also determined from SAXS measurements using two low-molecular-weight PS-*b*-P2VP and PS-*b*-P4VP copolymers.¹⁸ It is very interesting to observe in Figure 4b that values of α for P2VP/P4VP pair lies between those of PS/P4VP and PS/P2VP pairs.

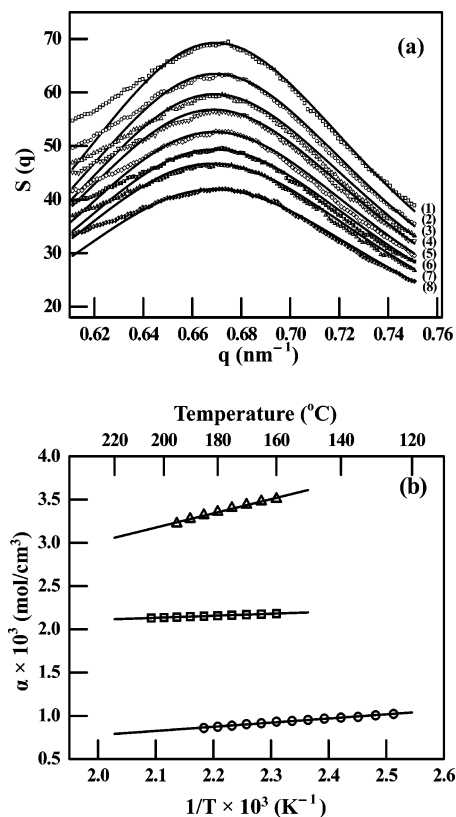


Figure 4. (a) Structure factor $S(q)$ for P24VP-LMW in the disordered state at various temperatures ($^{\circ}\text{C}$): (1) 160, (2) 165, (3) 170, (4) 175, (5) 180, (6) 185, (7) 195, and (8) 205. The solid lines are obtained by curve-fitting SAXS profiles to the RPA theory. (b) Plots of interaction parameter α vs $1/T$ (□) obtained from P24VP-LMW. For comparison, also shown are plots of α vs $1/T$ for PS/P2VP pair (○) and PS/P4VP pair (△).

Conclusions

In this study, we synthesized P2VP-*b*-P4VP copolymers with various molecular weights and block length ratios using anionic polymerization. P2VP-*b*-P4VP copolymers exhibited ODT upon heating, similar to PS-*b*-P2VP and PS-*b*-P4VP copolymers. This observation indicates that the repulsive force between P2VP and P4VP has increased significantly inducing the microphase separation even when the molecular weight of symmetric P2VP-*b*-P4VP copolymer was relatively low (~ 6000), even though the only difference between P2VP and P4VP is the position of nitrogen in the pyridine ring (ortho vs para positions). We have found that the values of α for P2VP/P4VP pair lie between those of PS/P4VP and PS/P2VP pairs.

Acknowledgment. This work was supported by the National Creative Research Initiative Program supported by Korean Organization of Science and Engineering Foundation (KOSEF). Small-angle X-ray scattering was performed at PLS beamline supported by POSCO and KOSEF.

Supporting Information Available: Figures of temperature dependence of depolarized light intensity and G' for P24VP-LO and P24VP-LD, SAXS profiles of P24VP-C, temperature dependence of depolarized light intensity for P24VP-C, and temperature dependence of depolarized light intensity and G' for P24VP-CO and P24VP-CD. This material is available free of charge via the Internet at <http://pubs.acs.org>.

References and Notes

- (1) Bates, F. S.; Fredrickson, G. H. *Annu. Rev. Phys. Chem.* **1990**, *41*, 525.

- (2) Leibler, L. *Macromolecules* **1980**, *13*, 1602.
- (3) Fredrickson, G. H.; Bates, F. S. *Annu. Rev. Mater. Sci.* **1996**, *26*, 501.
- (4) Hashimoto, T. In *Thermoplastic Elastomer*, 2nd ed.; Holden, G., Legge, N. R., Quirk, R., Schroeder, H. E., Eds.; Hanser: Munich, 1996; Chapter 15A.
- (5) Hamley, I. W., Ed. *Developments in Block Copolymer Science and Technology*; John Wiley & Sons Ltd.: Chichester, England 2004.
- (6) Schultz, M. F.; Khandpur, A. K.; Bates, F. S.; Almdal, K.; Mortensen, K.; Hajduk, D. A.; Gruner, S. M. *Macromolecules* **1996**, *29*, 2857.
- (7) Schultz, M. F.; Bates, F. S.; Almdal, K.; Mortensen, K. *Phys. Rev. Lett.* **1994**, *73*, 86.
- (8) Shull, K. R.; Kramer, E. J.; Hadziioannou, G.; Tang, W. *Macromolecules* **1990**, *23*, 4780.
- (9) Ruokolainen, J.; Mäkinen, R.; Torkkeli, M.; Mäkelä, T.; Serimaa, R.; ten Brinke, G.; Ikkala, O. *Science* **1998**, *280*, 557.
- (10) Ruokolainen, J.; Torkkeli, M.; Serimaa, R.; Komanshek, E.; ten Brinke, G.; Ikkala, O. *Macromolecules* **1997**, *30*, 2002.
- (11) Sohn, B. H.; Seo, B. H. *Chem. Mater.* **2001**, *13*, 1752.
- (12) Yun, S.; Yoo, S. I.; Jung, C. J.; Zin, W.; Sohn, B. *Chem. Mater.* **2006**, *18*, 5646.
- (13) de Moel, K.; Alberda van Ekenstein, G. O. R.; Nijland, H.; Polushkin, E.; ten Brinke, G. *Chem. Mater.* **2001**, *13*, 4580.
- (14) Valkama, S.; Kosonen, H.; Ruokolainen, J.; Haatainen, T.; Torkkeli, M.; Serimaa, R.; ten Brinke, G.; Ikkala, O. *Nat. Mater.* **2004**, *3*, 872.
- (15) Dai, K. H.; Kramer, E. J. *Polymer* **1994**, *35*, 157.
- (16) Clarke, C. J.; Eisenberg, A.; La Scala, J.; Rafailovich, M. H.; Sokolov, J.; Li, Z.; Qu, S.; Nguyen, D.; Schwarz, S. A.; Strzhemechny, Y.; Sauer, B. B. *Macromolecules* **1997**, *30*, 4184.
- (17) Alberda van Ekenstein, G. O. R.; Mayboom, R.; ten Brinke, G.; Ikkala, O. *Macromolecules* **2000**, *33*, 3752.
- (18) Zha, W.; Han, C. D.; Lee, D. H.; Han, S. H.; Kim, J. K.; Kang, J. H.; Park, C. *Macromolecules* **2007**, *40*, 2109.
- (19) Grosius, P.; Gallot, Y.; Skoulios, A. *Makromol. Chem.* **1970**, *136*, 191.
- (20) Bolze, J.; Kim, J.; Huang, J. Y.; Rha, S.; Youn, H. S.; Lee, B.; Shin, T. J.; Ree, M. *Macromol. Res.* **2002**, *10*, 2.
- (21) Balsara, N. P.; Perahia, D.; Safinya, C. R.; Tirrell, M.; Lodge, T. P. *Macromolecules* **1992**, *25*, 3896.
- (22) Balsara, N. P.; Dai, H. J.; Kesani, P. K.; Garatz, B. A.; Hammouda, B. *Macromolecules* **1994**, *27*, 7406.
- (23) Gouinlock, E. V.; Porter, R. S. *Polym. Eng. Sci.* **1977**, *17*, 535.

MA071120V